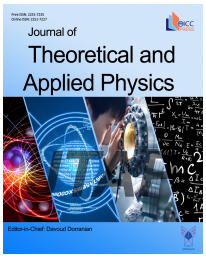

Volume 19, Issue 2, 192517 (1-7)

Journal of Theoretical and Applied Physics (JTAP)

https://doi.org/10.57647/j.jtap.2025.1902.17

Investigation of the structural and magnetical properties of polyaniline-nickel ferrite-carbon ternary composite layers

Zainab Jawad Jaber[1], Zhaleh Ebrahiminejad[2,*], Somayeh Asgary[2], Amir Hoshang Ramezani[2]

[1]*Faculty of Converging Sciences and Technologies, Department of Physics, Science and Research Branch, Islamic Azad University, Tehran, Iran.*
[2]*Department of Physics, West Tehran Branch, Islamic Azad University, Tehran, Iran.*

[*]**Corresponding authors:** zhl.ebrahimi@gmail.com

Original Research

Received:
30 November 2024
Revised:
2 January 2025
Accepted:
2 February 2025
Published online:
10 April 2025

Abstract:

In the present research, the production of polyaniline-nickel ferrite-carbon composite layers is discussed experimentally. The carbon nanoparticles were prepared by green synthesis method. The different properties of these nanoparticles were studied using different analyzes such as X-ray diffraction patterns, infrared absorption spectroscopy, scanning electron microscope images, vibrating sample magnetometry, and atomic force microscope analyzes. The copper substrate will be used to show this ternary components polyaniline-nickel ferrite-carbon and electrochemical method. The XRD pattern showed crystallinity nature for Nickel-ferrite nanoparticles. The results show that the saturation magnetization value for the polyaniline-nickel ferrite-carbon nanocomposite is 6 times bigger than the obtained value for nickel ferrite. The rod structure of carbon nanotubes shown in the AFM analysis indicated high surface roughness, which causes the waves to be captured by radars.

Keywords: Thin film; Roughness; Polyaniline; Ternary composite; Carbon nanoparticles

1. Introduction

During the last decades, experimental and theoretical results have shown that particle aggregation shows an significant role in regulating the material properties of colloidal systems. Investigation on the geometric properties of growth surfaces remains one of the greatest essential matters in the non-equilibrium statistical physics arena. Not only due to modeling the properties is a challenge for the theoretical physicist, but mainly to build and shape the surfaces with the desired goals [1–5].

In manufacturing procedures, the surface morphology can be pretentious by a wide variety of parameters. These sources include imprecisions in the machine tools, vibrations of the machine or workpiece, deformation under cutting forces, all of that will lead to irregularities on a millimetre scale, and material rupture during chip removal, which will lead to irregularities on a micro-scale. To put it another way, the surface morphology changes depending on the size. In a wide variety of technical applications, it is helpful to classify surface morphology as micrometer, millimeter, and meter-scale surface roughness, waviness, and lay, respectively. At the nanoscale (also known as the nanometer scale), surface roughness is connected with atomic structure, which is significant because it focuses on the position of a single atom. Surface phenomena, such as friction, adhesion, contact angle, light reflection and photon absorption are greatly influenced by the morphology of the surface. Research fields ranging from quality assurance and tribology (the study of friction, lubrication, and wear) to biomechanics and hydrodynamics, and even oceanography and selenology are among those in which roughness plays a significant role [1–5].

The shape of the structures because of the deposition of particles is a subject that has received a lot of attention and

has challenged theoretical and experimental investigators in the field of material physics. Experimentally, there is a physical possibility of thin film growth. Different models have been used to a great extent in this field of studies using different shapes of particles [6–12].

Although many models are much simpler, they can be used as a good starting point for study. More complex processes are directly related to the empirical growth process. New experimental techniques, such as molecular beam sputtering or coherent growth, can provide appropriate materials for many applications in various fields, such as medicine [13–16].

The properties of the thin layer at the sub-micron level and the mechanisms that determine the morphology of the thin layer can help in achieving better control of the properties of the thin layer in science and technology.

Inorganic nanomaterials composited with polyaniline (PANI) can improve the mechanical properties and extra properties reliant on the additives used. Conductive ferrite/polymer composites provide a new functional combination between organic and inorganic materials.

PANI coating on ferrite nanoparticles can increase compatibility with organic materials, decrease washing sensitivity and possibly prevent aggregation. Newly, several investigates have attentive on the PANI/ferrite composites to find the materials with synergetic or complementary behavior between PANI and ferrite nanoparticles [17–23]. Dopping polyaniline with magnetic particles have received lots of acknowledgment because of its vast application [24–29].

Polyaniline-nickel-ferrit nanocomposites with various contents of nickel-ferrit were synthesed by chemical oxidation polymerization method, while the nickel-ferrite nanoparticles were prepared by sol–gel technique [30]. The effects of adding nickel-ferrite nanoparticles on the magnetic and electrical properties of PANI were studied by Prasanna et al. [31]. From Singh et al. [32] study, in order to increase the electrochemical performance of PANI incorporated that with transition metal oxide (nickel-ferrite).

The polyaniline-ferrite-carbon composite can be a very suitable conductive and magnetic composite for applications such as anti-radar conductive coatings on aircraft and military bodies. Due to its high conductivity and magnetic properties, this composite can absorb radar waves and thus decrease the possibility of recognizing the identity and position of the aircraft for different radar systems. In addition, this composite can be used as a suitable alternative for high-performance magnetic and conductive composites in industrial and military applications.

Kolhar et al. [33] doped synthesed nickel-ferrite nanoparticles with polyaniline in various weight ratios using an in situ polymerization technique.

In the present research, the production of composite layers is discussed experimentally. The carbon nanoparticles is prepared by the green synthesis methodand which will be explained in the next section.

The experimental aim is to fabricate thin layers of transparent polyaniline with magnetic nickel ferrite materials and carbon nanoparticles. Then the structural and magnetical properties of this layer have been compared with nickel-ferrite thin layer. The different properties of prepared thin films were studied by using various analytical methods like X-ray diffraction patterns, infrared absorption spectroscopy, scanning electron microscope images, vibrating sample magnetometry, and atomic force microscope analysis. The organization of this paper is as follow: In section 2, the methodology and experimental setups have been explained. The results have been presented in section 3, and they have been summarized in section 4.

2. Methodology and experimental setups

2.1 The green synthesis of nanoparticles (NPs)

The green production of nanoparticles (NPs) is a bottom-up strategy that involves the synthesis of NPs via the oxidation/reduction procedure of metallic ions using organic moieties derived from biological resources. This process creates NPs. Microorganisms like bacteria, yeast, algae, fungi and actinomycetes could be part of these biological systems. Plant extracts from a variety of plants might also be included [34–36].

An advanced combination of citric acid and ethylene diamine has been used to make carbon nanoparticles. With a one-to-one stoichiometric ratio, both materials were added to the water solvent and placed inside the autoclave for 72 hours at a temperature of 220 ºC. After the completion of the reaction, a black precipitate containing carbon dots is obtained, which is washed several times using ethanol, acetone, and water. In the final step, the black powder is subjected to ultrasonic waves with a power of 400 watts to make the carbons.

To produce nickel-ferrite nanoparticles, 0.01 mol of hexavalent nickel nitrate (Nickel(II) nitrate hexahydrate Merck) and 0.02 mol of hexavalent iron nitrate (Iron(III) nitrate nonahydrate Merck) were first dissolved in 200 mL of deionized water. Then, 0.5 g of sodium dodecyl sulfate (Sodium dodecyl sulfate Merck) was added as a precipitating agent. In the end, 10 mL of one-molar ammonia (Ammonia solution 25% Merck) was added as a precipitant, and the pH was fixed at eleven. Then, the resulting solution was transferred to an autoclave and kept at a temperature of 200 ºC for 5 hours. After washing and centrifugation, it was dried in a vacuum oven at 80 ºC for 24 hours for sampling.

To manufacture carbon nanoparticles, an advanced combination of citric acid and ethylene diamine has been used. In this method, both substances were added to the water solvent in a stoichiometric ratio of one to one and placed in an autoclave for 72 hours at 220 ºC. After the reaction is complete, a black precipitate consisting of carbon dots is obtained, which is washed several times using ethanol, acetone, and water. In the final stage, to manufacture carbons, the black powder is placed under ultrasonic waves with a power of 400 watts.

2.2 Fabrication of polyaniline thin films

At first, carbon nanoparticles and nickel ferrite nanoparticles are made (section 2.1), and then they are dispersed in aniline using ultrasonic waves and placed inside the electrochemical cell. A few millilitres of sulfuric acid (Sulfuric acid, Merck) and phosphoric acid (H_3PO_3, Merck) will be used

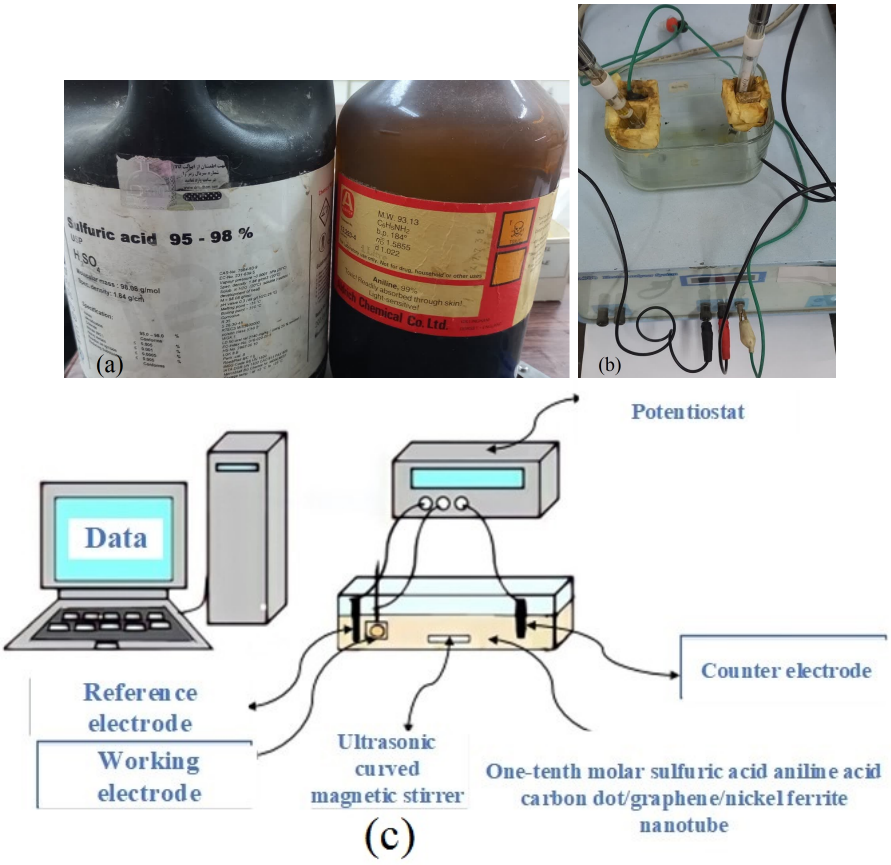

Figure 1. (a) Aniline (right), Sulfuric acid (left), (b) three electrodes from the right side, the yellow working electrode is copper, the middle red electrode is the reference electrode or calomel, and the black electrode is the Platinum electrode or counter, and (c) a schematic diagram of the layer deposition device.

to adjust the pH. A copper substrate is placed at the cathode electrode, where reduction occurs. The calomel electrode will be used as the reference electrode and the platinum electrode as the counter electrode. Aniline substrate will be placed in the form of polymer along with carbon nanoparticles and magnetic ferrite on the copper substrate, and after these steps, the materials include a copper substrate, aniline solution and nanoparticles beside three electrodes. Then the liquid and added nanoparticles are placed on the substrate. The wave absorption test has shown that this compound absorbs electromagnetic waves. The experimental setups for layer deposition are shown in figure 1.

Figure 1 (a) Aniline (right), Sulfuric acid (left), (b) three electrodes from the right side, the yellow working electrode is copper, the middle red electrode is the reference electrode or calomel, and the black electrode is the Platinum electrode or counter, and (c) a schematic diagram of the layer deposition device.

3. Results and discussions

This research aimed to make thin layers of conductive polyaniline along with magnetic nickel ferrite materials and carbon nanoparticles, which were prepared and synthesized by ultrasonic method. This layer is composed of three layers, the first layer (which is the ground) is polyaniline, the second layer is a magnetic material, which is nickel ferrite nanoparticles, and the third layer is an additive carbon nanoparticles.

3.1 X-ray diffraction analysis (XRD)

The X-ray diffraction pattern of nickel-ferrite nanoparticles and PANI are shown in figures 2 and 3. In figure 2, the pattern is totally consistent with the indices of pure standard materials. Nickel-ferrite nanoparticles showed crystallinity in tature with Miller indices of (220), (311), (400), (422), (511), (440) and (533) according to (JCPDS Card No. 74-2081). Figure 3 shows the X-ray diffraction diagram of polyaniline on copper substrate. The XRD spectra did not

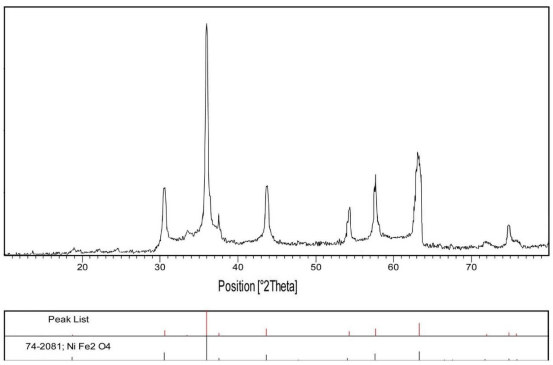

Figure 2. The X-ray diffraction pattern of nickel-ferrite nanoparticles.

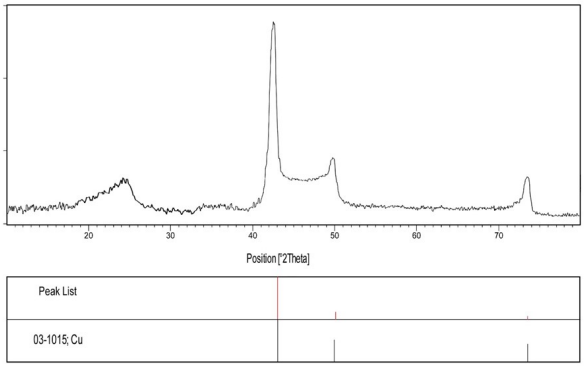

Figure 3. The X-ray diffraction pattern of polyaniline on copper substrate.

show any other peaks associated to PANI that shows amorphous nature for PANI except a broud peak at $2\theta = 25.2°$. Three strong peaks at $2\theta = 43°$, 54 and 70° associated to copper the Miller index (111), (200), (220) respectively. Khairy et al. [31] reported amorphous nature for pure PANI with two broud diffraction peaks at $2\theta = 20.3°$ and 25.1° according to (JCPDS Card No. 03-1015). From Kolhar et al. [37] and Pramanna et al. [32] study, crystalline nature for nickel-ferrites nanoparticles and amorphous nature for polyaniline is confirmed.

3.2 SEM characterization

Figure 4 respectively show the scanning electron microscope images of pure polyaniline, pure carbon and nickel-ferrite nanoparticles. These images were prepared with working distances of 1 magnetic nickel-ferrite nanoparticle 1.73 and 2.77, 4.61 and 39.5 µm, and scales of 500 nm and 1 µm.

3.3 Magnetometry of the vibrating sample

The magnetometric diagrams of the vibrating sample of nickel-ferrite magnetic nanoparticles and polyaniline-nickel ferrite-carbon ternary composite are shown in figures 5 and 6.

Magnetic properties of deposited samples strongly affected by grain size and the final compound. The magnetic properties change with magnetic moment, magnetization, and coercivity, is by reason of chemical stability effect. Magnetic properties of samples have been presented in figure. By hysteresis curves. Using hysteresis plot the amount of saturation magnetism for nickel-ferrite is around 30 emu/g, and for polyaniline-nickel-ferrite-carbon nanocomposite is around 0.5 emu/g. It can be seen that the saturation magnetization increase occures when it enters into both sides [38, 39]. The value of residual magnetism is zero for both photos. In VSM diagrams, the horizontal graph displays the hardness (or coercivity), and the vertical graph displays its magnetization.

Commonly, the magnetic performance and the magnetic values (M_s) of the nanocomposites can be also described by the equation $M_s = \Phi m_s$, wherever Φ is the volume fraction of the magnetic particles and m_s is defined as the saturation moment of a single particle [40, 41].

Polyaniline-nickel-ferrite-carbon nanocomposite have fewer magnetization than pure nickel-ferrite nanoparticles, that revenues the total magnetic performance of the nanocomposite can be modified depending on these two parameters [42].

According to Molakeri et al. [43] study, polyaniline indi-

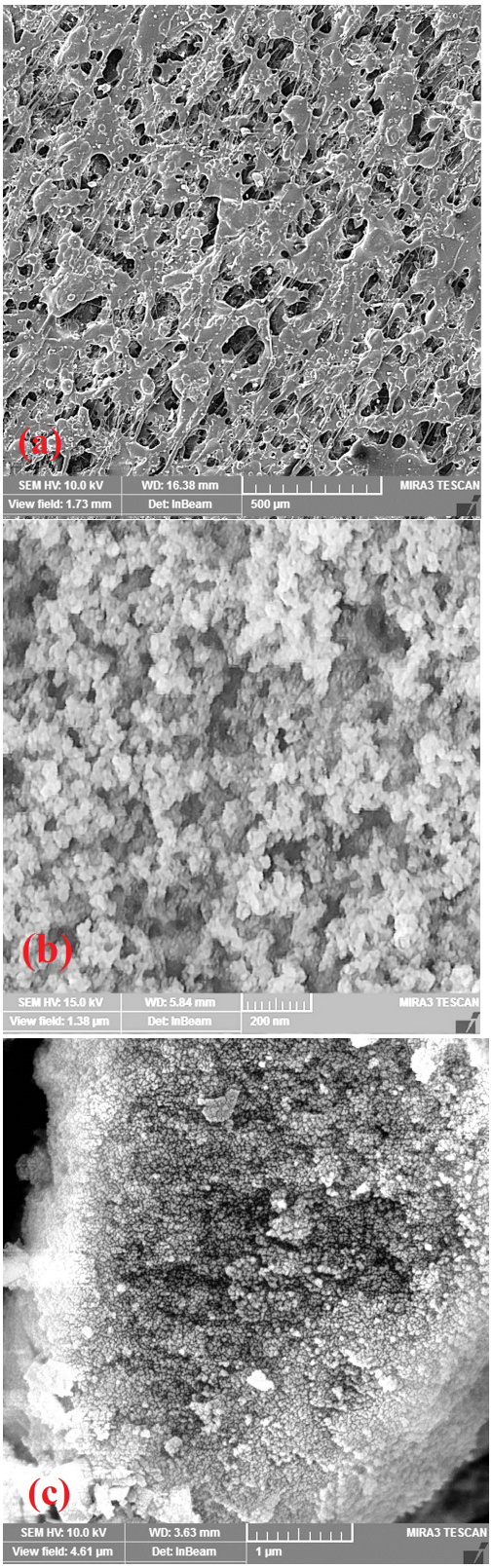

Figure 4. Scanning electron microscope images of (a) pure polyaniline, (b) pure carbon, and (c) nickel-ferrite nanoparticles.

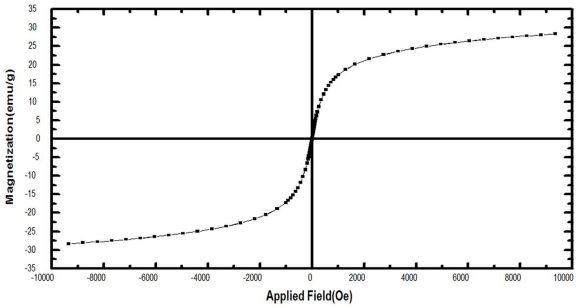

Figure 5. Vibrating sample magnetometry of pure ferrite-nickel nanoparticles.

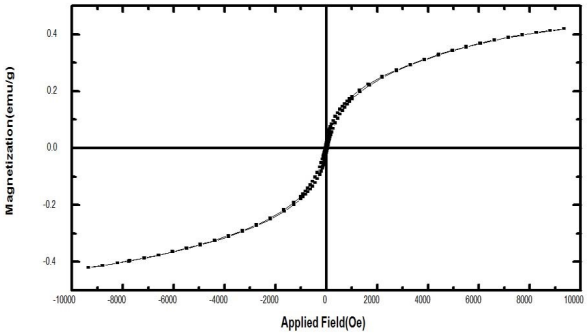

Figure 6. Magnetometry of vibrating three-layers polyaniline-nickel-ferrite-carbon composite sample.

cated diamagnetic behavior and nickel-ferrit particle and polyaniline-nickel-ferrit composites indicated ferromagnetic behavior. Patil et al. [44] showed that saturation magnetisation value for PANI-nickel-ferrit is 3.7 emu/g, that is lower than nickel-ferrit then, polyaniline-nickel-ferrit showed weak ferromagnetic behavior.

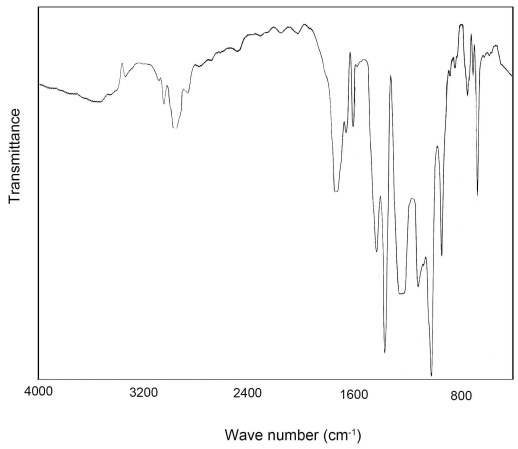

Figure 7. Infrared absorption spectroscopy of polyaniline.

3.4 Infrared (IR) absorption spectroscopy

The infrared absorption spectroscopy of polyaniline is shown in figure 7. For this substance, the peaks in the 3500 regions correspond to oxygen-hydrogen bonding, in the 3000 – 3200 region to carbon-hydrogen, the peak in the 1800 region to double carbon-oxygen, in the 1400 and 1000 region to carbon-oxygen, and in the 1300 region to carbon-oxygen. Double carbon shows carbon-carbon in the 1000 regions and iron-oxygen in the 500 regions.

3.5 Atomic force microscope (AFM) analysis

Atomic force microscope analysis of polyaniline-nickel ferrite-carbon ternary nanocomposite and nickel ferrite magnetic nanoparticles is shown in figure 8.
This analysis captures the elevations of the sample's surface (surface topography). The polyaniline-nickel ferrite-carbon nanocomposite is homogeneous and have smoother surface than nickel-ferrite.
AFM analysis is used to measure surface roughness, especially nanometer roughness. In the figures above, the protrusion is clearly visible, indicating the nanotubes' rod-like nature. The very issue of the rod and the roughness of the surface cause the waves to be trapped and detected, which causes them to return to the radar. Finally, we will conclude that nanotubes and polyaniline performed best.

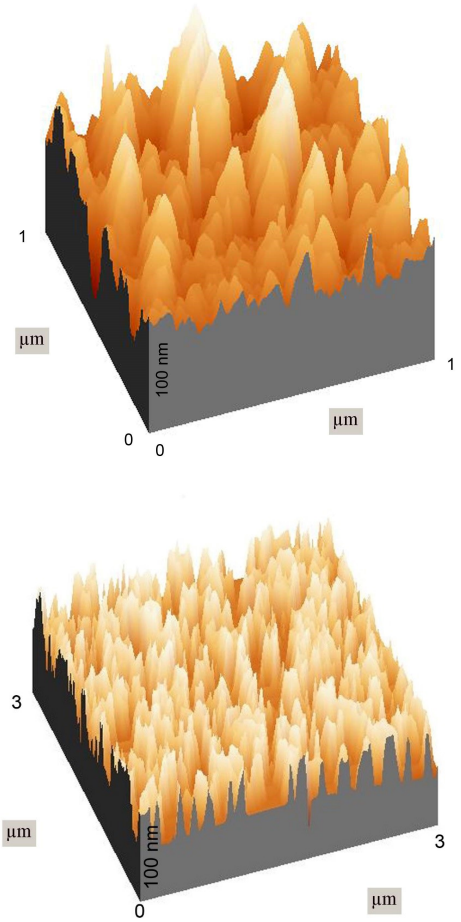

Figure 8. Infrared absorption spectroscopy of polyaniline.

4. Summary and concluding remarks

In the present work, the production of composite layers by different synthesis methods has been studied. Adding fine-grained magnetic materials such as nickel-ferrite nanoparticles to the polyaniline can improve the properties of the composite. The polyaniline-nickel-ferrite-carbon combination can be considered a new material with suitable properties for durable, magnetic and electrical applications at the industrial level. The crystallinity nature for Nickel-ferrite nanoparticles has been revaled by XRD pattern. The AFM analysis showed rod structure for carbon nanotubes with high surface roughness, which causes the waves to be captured by radars.

According to obtained results, the saturation magnetization value for the polyaniline-nickel ferrite-carbon nanocomposite is bigger around 6 times rather than nickel ferrite one. Various applications of this compound can include in making electronic components, magnetic sensors, electric vehicles, medical devices, etc.

Authors Contribution

All authors contributed to the study conception and design. Material preparation, data collection and analysis were performed by All authors. Also, the first draft of the manuscript was written by all author and they read and approved the final manuscript.

Availability of data and materials

Data sharing and data citation is encouraged.

The datasets generated during and/or analysed during the current study are available from the corresponding author on reasonable request.

The authors have no relevant financial or non-financial interests to disclose.

The authors declare that they have no known competing financial interests or personal relationships that could have appeared to influence the work reported in this paper.

All authors contributed to the study conception and design. Material preparation, data collection and analysis were performed by All authors. Also, the first draft of the manuscript was written by all author and they read and approved the final manuscript.

Conflict of interests

The authors declare that they have no known competing financial interests or personal relationships that could have appeared to influence the work reported in this paper.

References

[1] Z. Jardon, M. Hinderdael, J. Ertveldt, and P. Guillaume. "Production assessment of hybrid directed energy deposition manufactured sample with integrated effective structural health monitoring channel (eSHM). ". *Procedia Structural Integrity*, **34**:32–38, 2021. DOI: https://doi.org/10.1016/j.prostr.2021.12.005.

[2] Zh. Ebrahiminejad, S. F. Masoudis, R. S. Dariani, and S. S. Jahromi. "Thin film growth by using random shape cluster deposition.". *J. Chem. Phys.*, **137**:154703, 2012. DOI: https://doi.org/10.1063/1.4755956.

[3] C. Li, J. Zhang, J. Han, and B. Yao. "A numerical solution to the effects of surface roughness on water–coal contact angle.". *Scientific Reports*, **11**(1):459, 2021. DOI: https://doi.org/10.1038/s41598-020-80729-9.

[4] B. Bhushan. "Principles and applications of tribology.". *John Wiley & Sons*, 1999.

[5] T. R. Thomas. "Rough Surfaces. ". *Imperial College Press*, 1982.

[6] A.-L. Barabási and H. E. Stanley. "Fractal concepts in surface growth.". *Cambridge University Press*, 1995. DOI: https://doi.org/10.1017/CBO9780511599798.

[7] F. W. Bentrem, R. B. Pandey, and F. Family. "Roughening, deroughening, and nonuniversal scaling of the interface width in electrophoretic deposition of polymer chains.". *Physical Review E*, **62**: 914, 2000. DOI: https://doi.org/10.1103/PhysRevE.62.914.

[8] F. W. Bentrem, J. Xie, and R. B. Pandey. "Interface relaxation in electrophoretic deposition of polymer chains: Effects of segmental dynamics, molecular weight, and field.". *Physical Review E*, **65**: 41606, 2002. DOI: https://doi.org/10.1103/PhysRevE.65.041606.

[9] F. Family and T. s Vicsek. "Dynamics of fractal surfaces. ". *World Scientific*, 1991.

[10] P. Meakin. "Fractals, scaling and growth far from equilibrium.". *Cambridge University Press*, 1998.

[11] S. Mizani, R. Aliabadi, and H. Salehi. "Comparison of the effect of geometric shape and Cross-section of rod particles in biaxial and homeotropic phase formation. ". *Journal of Research on Many-body Systems*, **11**:56–67, 2021. DOI: https://doi.org/10.22055/JRMBS.2021.16783.

[12] E. Sharafedini, H. Hamzehpour, S. Farhad Masoudi, and M. Sahimi. "Electrical conductivity of the films grown by ballistic deposition of rodlike particles.". *Journal of Applied Physics*, **118**(21), 2015. DOI: https://doi.org/10.1063/1.4936548.

[13] S. Basrour and L. Robert. "X-ray characterization of residual stresses in electroplated nickel used in LIGA technique. ". *Materials Science and Engineering: A*, **288**:270–274, 2000. DOI: https://doi.org/10.1016/S0921-5093(00)00868-6.

[14] J. Volpp. "Behavior of powder particles on melt pool surfaces.". *The International Journal of Advanced Manufacturing Technology*, **102**: 2201–2210, 2019. DOI: https://doi.org/10.1007/s00170-018-03261-1.

[15] M. Rombouts, G. Maes, W. Hendrix, and E. Delarbre. "Surface finish after laser metal deposition.". *Physics Procedia*, **41**:810–814, 2013. DOI: https://doi.org/10.1016/j.phpro.2013.03.152.

[16] F. Forgerini and W. Figueiredo. "Random deposition of particles of different sizes.". *Physical Review E*, **79**(4):041602, 2009. DOI: https://doi.org/10.1103/PhysRevE.79.041602.

[17] G. Ćirić Marjanović. "Recent advances in polyaniline composites with metals, metalloids and nonmetals.". *Synthetic Metals*, **170**:31–56, 2013. DOI: https://doi.org/10.1016/j.synthmet.2013.02.028.

[18] C. Wang, Y. Shen, X. Wang, H. Zhang, and A. Xie. "Synthesis of novelNiZn-ferrite/polyaniline nanocomposites and their microwave absorptionproperties. ". *Mater. Sci. Semiconductor Proc.*, **16**:77–82, 2013. DOI: https://doi.org/10.1016/j.mssp.2012.06.015.

[19] P. Bhatt, R. B. Jotania, and R. Kumar. "Study of structural and magnetic properties of$(Co–Cu)Fe_2O_4$/PANI composites.". *Mater. Chem. Phys.*, **141**:406–415, 2013. DOI: https://doi.org/10.1016/j.matchemphys.2013.05.034.

[20] M. B. Mohamed and K. El-Sayed. "Structural, magnetic and dielectric propertiesof PANI-$Ni_{0.5}Zn_{0.5}Fe_{1.5}Cr_{0.5}O_4$ namocomposite.". *Composites Part B*, **56**:270–278, 2014. DOI: https://doi.org/10.1016/j.compositesb.2013.08.038.

[21] V. Babayan, N. E. Kazantseva, I. Sapurina, R. Moučka, J. Vilčáková, and J. Stejskal. "Magnetoactive feature of in-situ polymerized polyaniline film developedon the surface of manganese-zinc ferrite.

[22] H. Sozeri, U. Kurtan, R. Topkaya, A. Baykal, and M. S. Toprak. "Polyaniline (PANI)-$Co_{0.5}Mn_{0.5}Fe_2O_4$ nanocomposite: synthesis characterization and magneticproperties evaluation.". *Ceram. Int.*, **39**:5137–5143, 2013.
DOI: https://doi.org/10.1016/j.ceramint.2012.12.009.

[23] H. D. Kyomuhimbo and U. Feleni. "Electroconductive green metal-polyaniline nanocomposites: synthesis and application in sensors. ". *Electroanalysis*, **35**:202100636, 2023.
DOI: https://doi.org/10.1002/elan.202100636.

[24] S. Khan and Sh. Peshoria. "Polyaniline nanocomposites with doped ferrites as an electromagnetic shield.". *International Journal of Development Research*, **4**:1371–1376, 2014.
DOI: https://doi.org/10.37118/ijdr.

[25] M. T. Ramesan. "Synthesis and characterization of magnetoelectric nanomaterial composed of Fe_3O_4 and polyindole. ". *Advances in Polymer Technology*, **32**:21362, 2013.
DOI: https://doi.org/10.1002/adv.21362.

[26] M. T. Ramesan and K. Surya. "Synthesis, characterization, and properties of cashew gum graft poly(acrylamide)/magnetite nanocomposites.". *Journal of Applied Polymer Science*, **133**:5431–5438, 2016.
DOI: https://doi.org/10.1002/app.43496.

[27] P. Jayakrishnan and M. T. Ramesan. "Synthesis, structural, magneto-electric and thermal properties of poly (anthranilic acid)/magnetite nanocomposites.". *Polymer Bulletin*, **74**:3179–3198, 2017.
DOI: https://doi.org/10.1007/s00289-016-1883-0.

[28] P. Jayakrishnan, K. KJithin, K. Meera, and M. T. Ramesan. "Synthesis, characterization, magnetoelectric properties and gas sensing application of Poly(anthranilic acid-co-indole)/ magnetite nanocomposites.". *Journal of Thermoplastic Composite Materials*, **36**(6): 2523–2542, 2023.
DOI: https://doi.org/10.1177/08927057221098969.

[29] T. Anjitha, T. Anilkumar, G. Mathew, and M. T. Ramesan. "Zinc ferrite @ polyindole nanocomposites: Synthesis, characterization and gas sensing applications. ". *Polymer Composites*, **40**(7):2802–2811, 2019.
DOI: https://doi.org/10.1002/pc.25088.

[30] M. Khairy and M. E. Gouda. "Electrical and optical properties of nickel ferrite/polyaniline nanocomposite.". *Journal of Advanced Research*, **6**:555–562, 2015.
DOI: https://doi.org/10.1016/j.jare.2014.01.009.

[31] G. D. Prasanna, R. L. Ashok, and H. S. Jayanna. "Synthesis and characterization of magnetic and conductive nickel ferrite–polyaniline nanocomposites. ". *Journal of Cmposite Material*, **49**(21), 2014.
DOI: https://doi.org/10.1177/0021998314552090.

[32] G. Singh, Y. Kumar, and S. Husain. "Nickel ferrite doped polyaniline composites: Synthesis and analysis for a high-performance symmetric pseudo-supercapacitor.". *Energy Storage*.
DOI: https://doi.org/10.1002/est2.525.

[33] P. Kolhar, B. Sannakki, M. Verma, S. V. Prabhakar, and M. Alshehri. "Synthesis, characterization and investigation of optical and electrical properties of polyaniline/nickel ferrite composites.". *Nanomaterials*, **13**(15):2223, 2023.
DOI: https://doi.org/10.3390/nano13152223.

[34] Y. K. Gautam, K. Sharma, S. Tyagi, A. Kumar, and B. Pal Singh. "Chapter 6 - Applications of green nanomaterials in coatings.". *Green Nanomaterials for Industrial Applications*, 2022.
DOI: https://doi.org/10.1016/B978-0-12-823296-5.00014-9.

[35] D. N. Chandrani, S. Ghosh, and A. R. Tanna. "Green synthesis for fabrication of cobalt ferrite nanoparticles with photocatalytic dye degrading potential as a sustainable effluent treatment strategy. ". *Journal of Inorganic and Organometallic Polymers and Materials*, **34**:3100–3114, 2024.
DOI: https://doi.org/10.1007/s10904-023-02981-6.

[36] A. Chaudhari, T. Kaida, H. B. Desai, S. Ghosh, R. P. Bhatt, and A. R. Tanna. "Dye degradation and antimicrobial applications of manganese ferrite nanoparticles synthesized by plant extracts.". *Chemical Physics Impact*, **5**:100098, 2022.
DOI: https://doi.org/10.1016/j.chphi.2022.100098.

[37] Vadiraj K. T. and S. L. Belagali. "Characterization of polyaniline for optical and electrical properties.". *IOSR Journal of Applied Chemistry*, (**8**):1, 2015.
DOI: https://doi.org/10.9790/5736-0801025356.

[38] N. Yadav, A. Kumar, P. S. Rana, D. S. Rana, M. Arora, and R. P. Pant. "Finite size effect on Sm^{3+} doped $Mn_{0.5}Zn_{0.5}SmxFe_{2-x}O_4$ ($0 \leq x \leq 0.5$) ferrite nanoparticles.". *Ceram. Int.*, **41**:8623–8629, 2015.
DOI: https://doi.org/10.1016/j.ceramint.2015.03.072.

[39] K. Jalaiah and K. Vijaya Babu. "Structural, magnetic and electrical properties of nickel doped Mn-Zn spinel ferrite synthesized by sol-gel method. ". *J. Magn. Magn Mater*, **423**:275–280, 2017.
DOI: https://doi.org/10.1016/j.jmmm.2016.09.114.

[40] L. Li, Ch. Xiang, X. Liang, and B. Hao. "$Zn_{0.5}Cu_{0.4}Cr_{0.5}Fe_{1.46}Sm_{0.04}$ ferrite and itsnanocomposites with polyaniline and polypyrolle: preparation and electro-magnetic properties.". *Synth. Met.*, **160**:28–34, 2010.
DOI: https://doi.org/10.1016/j.synthmet.2009.09.026.

[41] R. M. Khafagy. "Synthesis, characterization, magnetic and electrical propertiesof the novel conductive and magnetic polyaniline/MgFe2O4 nanocomposite having the core–shell structure. ". *J. Alloys Compd.*, **509**:9849–9857, 2011.
DOI: https://doi.org/10.1016/j.jallcom.2011.07.008.

[42] Q. Song and Z. J. Zhang. "Shape control and associated magnetic properties of spinelcobalt ferrite nanocrystals.". *J. Amer. Chem. Soc.*, **126**:6164–6168, 2004.
DOI: https://doi.org/10.1021/ja049931r.

[43] A. K. S. Molakeri, A. D. Shetkar, B. Raghunanda, and S. Kalyane. "Electrical and magnetic properties of polyaniline-nickel ferrite composites.". *International Journal on Emerging Technologies*, **7**(2): 164–168, 2016.
DOI: https://doi.org/10.1166/jap.2017.1308.

[44] M. R. Patil and V. S. Shrivastava. "Adsorption of malachite green by polyaniline–nickel ferrite magnetic nanocomposite: an isotherm and kinetic study.". *Appl Nanosci*, **5**:809–816, 2015.
DOI: https://doi.org/10.1007/s13204-014-0383-5.